Electronic Supplementary Information

Tandem metathesis depolymerization and cyclopolymerization toward flexible-rigid block copolymer with unique damping properties

Lingli Zhang, Ying Quan, Hao Wang, Huijing Han, Xiaojuan Liao, Ruyi Sun* and Meiran Xie*

School of Chemistry and Molecular Engineering, East China Normal University, Shanghai 200241, China.

E-mail: rysun@chem.ecnu.edu.cn, mrxie@chem.ecnu.edu.cn

The following sections are included in the ESI:

Section 1. Experimental details for synthetic procedures

Syntheses of monomers

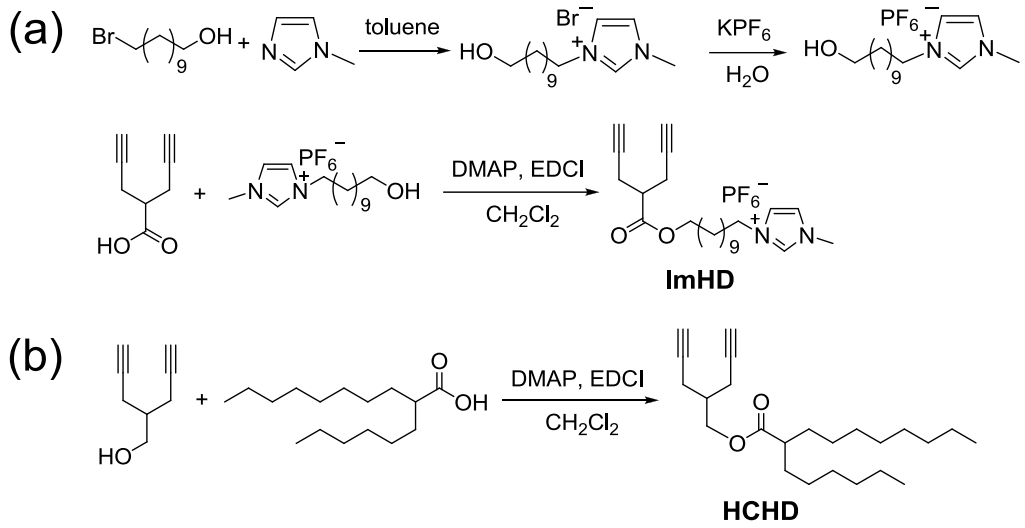

Scheme S1. Syntheses of 1,6-heptadiyne monomers containing imidazolium (a) and branched alkyl (b) groups.

Synthesis of 1-methyl-3-(11-hydroxy undecyl) imidazolium hexafluorophosphate: Under a nitrogen atmosphere, a mixture of 11-bromo-1-undecanol (7.91 g, 31.5 mmol) and 1-methylimidazole (2.47 g, 30 mmol) was dissolved in 20 mL of toluene and stirred at 80 ^{o}C for 2 h and at 110 ^{o}C for 2 h. The top phase was decanted, and the rest of the viscous liquid was washed with ethyl acetate repeatedly. The residual solvent was evaporated under vacuum to give a solid white power 1-methyl-3-(11-hydroxy undecyl) imidazolium bromide in 96% yield (9.58 g, 28.7 mmol). ^{1}H NMR (500 MHz, DMSO-d_6, ppm): δ 9.18 (s, 1H, NC*H*NCH$_3$), 7.79 (s, 1H, NC*H*CH), 7.72 (s, 1H, NC*H*CH), 4.32 (s, 1H, CH$_2$O*H*), 4.17-4.14 (t, 2H, CHC*H*$_2$O), 3.91-3.85 (s, 3H, NC*H*$_3$), 3.37-3.33 (m, 2H, CHC*H*$_2$CH), 1.80-1.74 (m, 2H, CH$_2$C*H*$_2$CH$_2$), 1.40-1.36 (m, 2H, CH$_2$C*H*$_2$CN), 1.26-1.24 (s, 14H, CH$_2$C*H*$_2$CH$_2$); ^{13}C NMR (125 MHz, DMSO-d_6, ppm): δ 136.95, 124.05, 122.72, 61.14, 49.92, 39.74, 36.23, 32.99, 29.85, 29.51, 29.40, 29.36, 29.27, 28.83, 25.97, 25.95. No further purification was made and it was used directly for the replacement of the Br^- by PF_6^- as follows. To a stirred solution of 1-methyl-3-(11-hydroxy undecyl) imidazolium bromide (10 g, 30 mmol) in 30

mL of H_2O, KPF_6 (6.63 g, 36 mmol) in 100 mL of H_2O was dropwise at 0 ºC over 1 h. Followed by stirring at room temperature for 24 h, the top phase was extracted with CH_2Cl_2. Then the organic phase was dried over anhydrous $MgSO_4$, which was concentrated under reduced pressure, and the solid was dried in vacuum to give white needle crystalline in 79% yield (9.4 g, 23.6 mmol). Ionic compound 1-methyl-3-(11-hydroxy undecyl) imidazolium hexafluorophosphate was synthesized, as shown in Scheme S1. ^{1}H NMR (500 MHz, DMSO-d_6, ppm): δ 9.18 (s, 1H, NC*H*NCH$_3$), 7.79 (s, 1H, NC*H*CH), 7.72 (s, 1H, NC*H*CH), 4.32 (s, 1H, CH$_2$O*H*), 4.17-4.14 (t, 2H, CHC*H*$_2$O), 3.91-3.86 (s, 3H, NC*H*$_3$), 3.37-3.33 (m, 2H, CHC*H*$_2$CH), 1.80-1.74 (m, 2H, CH$_2$C*H*$_2$CH$_2$), 1.40-1.36 (m, 2H, CH$_2$C*H*$_2$CN), 1.26-1.24 (s, 14H, CH$_2$C*H*$_2$CH$_2$); ^{13}C NMR (125 MHz, DMSO-d_6, ppm): δ 136.93, 124.06, 122.71, 61.17, 49.24, 36.20, 32.99, 29.93, 29.83, 29.51, 29.41, 29.33, 29.27, 28.82, 25.97, 25.94; ^{19}F NMR (125 MHz, DMSO-d_6, ppm): δ -69.38, -70.90.

*Synthesis of 4-(1-methyl-3-undecyl imidazolium hexafluorophosphate) ester-1,6-heptadiyne (**ImHD**)*: Under a nitrogen atmosphere, *1-methyl-3-(11-hydroxy undecyl) imidazolium* hexafluorophosphate (5.98 g, 15 mmol) were disolved in 10 mL of anhydrous CH2Cl2, 4-(carboxylic acid)-1,6-heptadiyne (2.15 g, 15.8 mmol) and DMAP (0.55 g, 4.5 mmol) were added under stirring at ice-water bath for 15 min, then EDCI•HCl (3.74 g, 19.5 mmol) was added to the mixture, stirred at room temperature for 36 h. After the reaction was completed, the resulting mixture was washed with saturated salt solution. The filtrate was concentrated and purified by column chromatography on silica gel using CH_2Cl_2/CH_3OH (40:1) as eluent. The colorless viscous liquid 4-(1-methyl-3-undecyl imidazolium hexafluorophosphate) ester-1,6-heptadiyne (**ImHD**) (2.8 g, 93%) was obtained. ^{1}H NMR (500 MHz, $CDCl_3$, ppm): δ 8.52 (s, 1H, NC*H*NCH$_3$), 7.32-7.31 (s, 2H, NC*H*CH), 4.17-4.13 (m, 4H, CC*H*$_2$CH$_2$), 3.39 (s, 3H, NC*H*$_3$), 2.85-2.75 (s, 1H, COOC*H*$_2$), 2.70-2.60 (m, 4H, C*CH*$_2$CH), 2.01 (t, 2H, C*H*CCH),1.91-1.77(t, 2H, CH$_2$C*H*$_2$CH$_2$), 1.66-1.53(m, 2H, CH$_2$C*H*$_2$CH$_2$) 1.36-1.17(m, 16H,

$CH_2CH_2CH_2$); ^{13}C NMR (125 MHz, $CDCl_3$, ppm): δ 171.78, 135.31, 123, 121.4, 79.9, 69.92, 64.59, 49.54, 42.44, 35.63, 29.29, 28.65, 28.25, 27.92, 25.53, 25.18, 19.3; ^{19}F NMR (125 MHz, $CDCl_3$, ppm): δ -71.3, -73.06.

*Synthesis of 4-(2-hexyldecyl carbonyloxymethyl)-1,6-heptadiyne (**HCHD**)*: To a solution of 4-hydroxymethyl-1,6-heptadiyne (0.64 g, 5.25 mmol) in 5 mL of anhydrous CH_2Cl_2, 2-hexyldecanoic acid (1.63 g, 12 mmol) and DMAP (0.18 g, 1.5 mmol) were added under stirring at ice-water bath for 5 min, then EDCI•HCl (1.25 g, 6.5 mmol) was added to the mixture, stirred at room temperature for 3 days. The solvent was removed under reduced pressure. The solid was purified by column chromatography on silica gel using CH_2Cl_2/CH_3OH (40:1) as eluent. The light yellow liquid 4-(2-hexyldecyl carbonyloxymethyl)-1,6-heptadiyne (**HCHD**) (1.4 g, 78%) was obtained. ^1H NMR (500 MHz, $CDCl_3$, ppm): δ 4.15-4.14 (d, 2H, $CHCH_2O$), 2.39-2.37 (m, 4H, $CH{\equiv}CCH_2CH$), 2.35-2.31 (m, 1H, CH_2CHCH_2), 2.16-2.11 (m, 1H, $COCHCH_2$), 2.00 (t, 2H, $C{\equiv}CH$), 1.62-1.4 (m, 4H, $CHCH_2CH_2$), 1.61-1.23 (m, 20H, $CH_2CH_2CH_2$ + $CH_2CH_2CH_3$), 0.88-0.86 (t, 6H, CH_2CH_3). ^{13}C NMR (125 MHz, $CDCl_3$, ppm): δ 176.48, 81.01, 70.52, 64.87, 45.96, 36.64, 32.68, 32.01, 29.72, 29.4, 27.58, 22.8, 19.99, 14.21.

Syntheses of homopolymers via MCP

*Synthesis of homopolymer **PImHD**$_{100}$*: A 25 mL Schlenk flask was charged with monomer **ImHD** (258.2 mg, 0.5 mmol) dissolved in 4 mL of $CHCl_3$. In another 25 mL flask, **Ru-III** (4.4 mg, 5 μmol) and 3,5-dichloropyridine (7.4 mg, 50 μmol) were dissolved in 1 mL of $CHCl_3$. After being degassed with three freeze-vacuum-thaw cycles, the catalyst solution was then injected into the pre-heated monomer solution via a syringe under vigorous stirring at 30 ^oC for 1 h. The resultant homopolymer was insoluble and precipitated out from the reaction system as a purple solid after polymerization within 1 min. Then an excess of vinyl ethyl ether was added to the mixture and stirring for another 1 h. The solid was washed with

methanol and dried under vacuum to afford **PImHD**$_{100}$ as a purple solid (52 mg, 21%). ^{1}H NMR (600 MHz, (DMSO-d_6, ppm): δ 9.06 (s, 1H, CNC*H*CN), 7.69 (d, 2H, CN*CH*CH), 6.80 (s, 2H, CH_2=C*H*CH), 4.11 (t, 4H, CO*CH*$_2$$CH_2$, CN*CH*$_2$$CH_2$), 3.83 (s, 3H, CNC*H*$_3$), 2.92 (s, 5H, *CCH*$_2$CH, CH_2*CH*CO), 1.86-0.96 (m, 18H, *C*H_2*CH*$_2$$CH_2$). ^{13}C NMR (150 MHz, DMSO-d_6, ppm): δ 175.36, 138.26, 136.42, 123.59, 123.27, 122.2, 64.21, 48.77, 37.03, 35.72, 29.40, 29.01, 28.9, 28.72, 28.46, 28.18, 25.57, 25.40.

Synthesis of homopolymer ***PHCHD***$_{100}$: A 25 mL Schlenk flask was charged with monomer **HCHD** (180 mg, 0.5 mmol) dissolved in 3 mL of $CHCl_3$. In another 25 mL flask, **Ru-III** (4.4 mg, 5 μmol) and 3,5-dichloropyridine (7.4 mg, 50 μmol) were dissolved in 2 mL of $CHCl_3$. After being degassed with three freeze-vacuum-thaw cycles, the catalyst solution was then injected into the pre-heated monomer solution via a syringe under vigorous stirring at 30 ^{o}C for 1 h. Then an excess of vinyl ethyl ether was added to the mixture and stirring for another 1 h. The solution was precipitated into methanol and dried under vacuum to afford homopolymer **PHCHD**$_{100}$ as a purple solid (140 mg, 78%). ^{1}H NMR (600 MHz, $CDCl_3$, ppm): δ 6.70 (s, 2H, C*H*CH=CH), 4.13-4.12 (s, 2H, CHC*H*$_2$CO), 3.17-2.25 (m, 6H, O=CC*H*CH_2 + CH_2C*H*CH_2 + CHC*H*$_2$$CH_2$), 1.62-1.47 (s, 2H, CHC*H*$_2$$CH_2$), 1.27 (s, 20H, CH_2C*H*$_2$$CH_2$), 0.99-0.83 (m, 6H, CH_2C*H*$_3$). ^{13}C NMR(150 MHz, $CDCl_3$, ppm): δ 176.72, 138.80, 123.37, 67.57, 46.02, 37.01, 34.82, 32.74, 32.02, 31.88, 29.83, 29.45, 27.71, 22.82, 14.21.

Syntheses of modifier

Synthesis of 4-(9-bromoheptadecyl)-1,2,4-triazoline-3,5-dione ***(BrTAD)***: oleic acid (22.03 g, 80 mmol) and toluene (120 mL) were charged into a 500 mL round-bottom flask equipped with a magnetic stirrer under nitrogen atmosphere, and the mixture was stirred at room temperature for 1 h. Diphenylphosphoryl azide (24.2 g, 88 mmol) and triethylamine (22 mL) were added to the solution and refluxed at 100 ^{o}C for 3 h. Next, a solution of ethyl carbazate

(12.5 g, 120 mmol) in toluene (120 mL) was added. The mixture was stirred for 6 h at 90 ºC. The mixture was concentrated in vacuum and purified by water and methanol to give the product 8-ene-heptadecyl-1-carbethoxysemicarbazide (**HD-CSC)** as a powder (29.9 g, 78.1 mmol) in a yield of 97.6%.

A 500 mL round-bottom flask was charged with **HD-CSC** (30 g, 80 mmol) dissolved in the aqueous KOH solution (4 mol L^{-1}, 60 mL). The mixture was refluxed at 100 ºC for 2 h, then cooled to room temperature, and acidified until pH=1 by the addition of hydrogen chloride (6 mol L^{-1}). The combined solution was concentrated, and the residual was then redissolved in CH_2Cl_2, followed by drying with $MgSO_4$. The mixture was filtered off, concentrated under reduced pressure, and dried in a vacuum to give the product 8-ene-heptadecyl-1,2,4-urazole (**HD-UZ**) as light yellow waxy solid (25.3 g, 75 mmol) in a yield of 93.6%. ^{1}H NMR (500 MHz, $CDCl_3$, ppm): δ 7.9 (s, 2H, O=CNH), 5.37-5.32 (m, 2H, CH_2*CH*CH), 3.51-3.14 (m, 2H, CHC*H*$_2$N), 2.02-1.97 (m, 4H, CHC*H*$_2$CH$_2$), 1.39-1.23 (m, 22H, CHC*H*$_2$CH$_2$ + CH_2C*H*$_2$CH$_3$), 0.89-0.86 (t, 3H, CH_2*CH*$_3$). ^{13}C NMR (125 MHz, $CDCl_3$, ppm): δ 156.16, 139.26, 114.33, 41.0, 39.45, 33.91, 30.14, 29.47, 29.25, 29.01, 28.12, 27.02, 26.81.

HD-UZ (1 g, 3 mmol), N-bromosuccinimide (2.4 g, 15 mmol), and CH_2Cl_2 (3 mL) were charged into a 25 mL round-bottom flask equipped with a magnetic stirrer under nitrogen atmosphere and stirred for 2 h in an ice bath. The reaction mixture was filtered off, concentrated, and then dissolved in petroleum ether, centrifugation, and filtration. The filtrate was concentrated under reduced pressure, and the solid was dried in vacuum to give the bright red mucus product 4-(9-bromoheptadecyl)-1,2,4-triazoline-3,5-dione (**BrTAD**) (1.1 g, 2.6 mmol) in a yield of 88%. ^{1}H NMR (500 MHz, DMSO-d_6, ppm): δ 4.38 (dd, 2H, CH_2C*H*$_2$N), 3.46 (t, 1H, BrC*H*CH$_2$), 1.88 (m, 4H, CHC*H*$_2$CH$_2$), 1.68-0.98 (m, 24H, C*H*$_2$CH$_3$ + CH_2C*H*$_2$CH$_2$), 0.86 (t, 3H, CH_2*CH*$_3$). ^{13}C NMR (125 MHz, DMSO-d_6, ppm): δ 160.13,

61.49, 42.52, 36.69, 31.23, 30.46, 28.77, 28.56, 28.25, 26.82, 25.85, 22.08, 13.94. HR-MS (ESI^+): m/z calcd for $C_{19}H_{33}BrN_3NaO_2$ $[M+Na]^+$: 437.2138, found: 437.2152.

Synthesis and TAD-modification of triblock copolymer: ***d*NR$_{x2}$-*b*-PHCHD$_{100}$-*b*-PImHD$_{50}$** (52 mg, 0.4 mmol) and $CHCl_3$ (2 mL) were charged into a 25 mL of round-bottom equipped with a magnetic stirrer and stirred at room temperature until the solids are dissolved. Then, a solution of **BrTAD** (16.6 mg, 0.04 mmol) in 1 mL of CHCl3 was added to the mixture and stirred for 2 h. The solution was precipitated into methanol and stirring for hours. The reaction mixture was filtered off, and the soft solid was washed with methanol for 2 times and dried in vacuum to give the product (***d*NR$_{x2}$-*b*-PHCHD$_{100}$-*b*-PImHD$_{50}$)-X%BrUZ** as a purple solid (62 mg, 90%). ^{1}H NMR (600 MHz, THF-d_8, ppm): δ 10.828 (s, O=CNHN), 8.09 (s, CNC*H*CN), 7.47-7.43 (d, CN*CH*CH), 6.89-6.708 (m, trans-C=CH on **PHCHD** and **PImHD** backbone), 5.502 (s, C=C*H* on ***d*NR$_{x2}$** backbone), 5.324-4.649 (m,), 4.298-3.810 (m, NCH_2CH$_2$ + CH$_2$C*H*NNH + O=COCH_2CH + O=COCH_2CH$_2$), 3.69 (s, NCH_3), 3.449 (s, BrC*H*CH$_2$), 3.257-1.826 (CH$_2$C*H*C=CH + BrCHCH_2CH$_2$ + CHCH_2CH$_2$CH$_2$+ CH$_2$C*H*CH$_2$O + OOC=C*H*CH$_2$ + CH$_2$C*H*C=O), 1.61-1.10 (CH$_3$CHCH_2 + BrCHCH$_2$CH_2 + O=CCHCH_2 + CH$_2$CH_2 CH$_2$ + O=CCHCH$_2$CH_2), 0.887 (m, CH$_2$CHCH_3 + CH$_2$CH$_2$CH_3 + CH=CCHCH_3).

Section 2. Data and results

1. Characteristics of homopolymers and block copolymers

Structure characterization of monomers

The monomers **HCHD** and **ImHD** were synthesized and characterized. In the ^{1}H NMR spectrum (Fig. S1a), the integration ratio of the terminal acetylenic proton (H_a) at 2.03 ppm to the proton on imidazole ring (H_j) at 8.52 ppm was about 1:1. Meantime, the ^{19}F NMR spectrum of **ImHD** (Fig. S1c) showed the resonance signals of PF_6^- group at -71.3 and -73.06 ppm, which confirmed the quantitative reaction of the monomer. Similarly, the ^{1}H NMR

spectra of **HCHD** showed the integration ratio of the terminal acetylenic proton (H_a) at 2.00 ppm to the tertiary carbon protons (H_e) at 2.14 ppm was about 1:1 (Fig. S2a), which also means the success of the esterification reaction for the syntheses of **HCHD**.

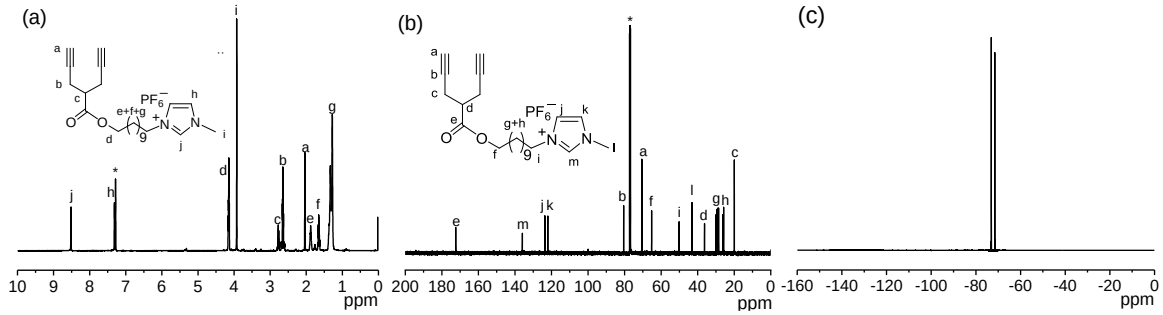

Fig. S1 ^{1}H (a) ,^{13}C (b) and ^{19}F (c) NMR spectra of **ImHD** in $CDCl_3$.

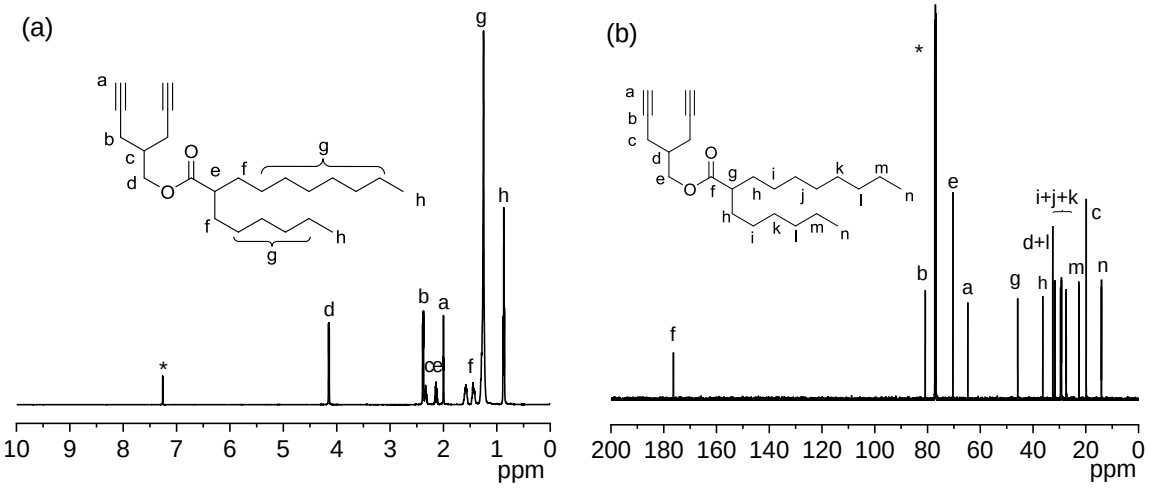

Fig. S2 ^{1}H (a) and ^{13}C (b) NMR spectra of **HCHD** in $CDCl_3$.

Characteristics of homopolymers and triblock copolymers

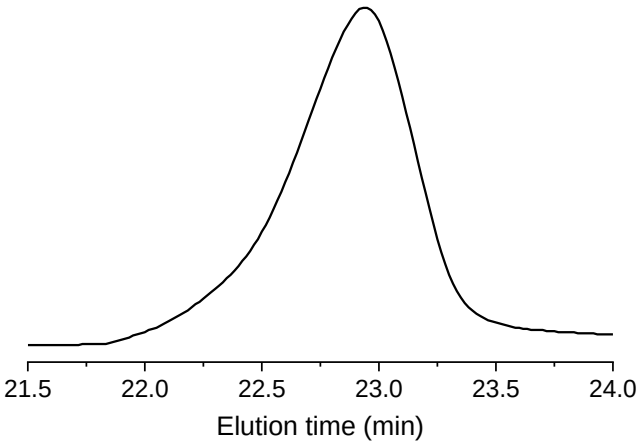

Fig. S3 GPC trace of homopolymer **PImHD**$_{100}$ in DMF.

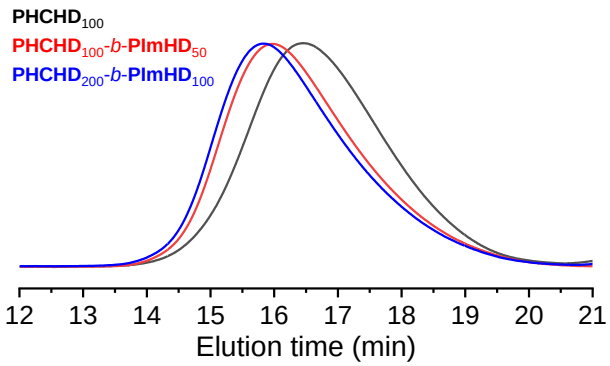

Fig. S4 GPC traces of homopolymer and diblock copolymers in THF.

Table S1. Solubility of polymers in various solvents at room temperature.*

Sample	MeOH	CH_2Cl_2	$CHCl_3$	THF	DMF	acetone	toluene
PImHD$_{100}$	–	–	–	–	+	–	–
PHCHD$_{100}$	–	+	+	+	–	+–	+–
PHCHD$_{100}$-*b*-**PImHD**$_{50}$	–	+	+	+	+–	+–	+–
***d*NR**-*b*-**PHCHD**$_{100}$-*b*-**PImHD**$_{50}$	–	+	+	+	+–	+–	+–
(***d*NR**$_{x2}$-*b*-**PHCHD**$_{100}$-*b*-**PImHD**$_{50}$)-40%**BrUZ**	–	+	+	+	–	–	–

*1 mg of polymers in 1 mL of solvent. –: insoluble; +–: partially soluble; +: soluble.

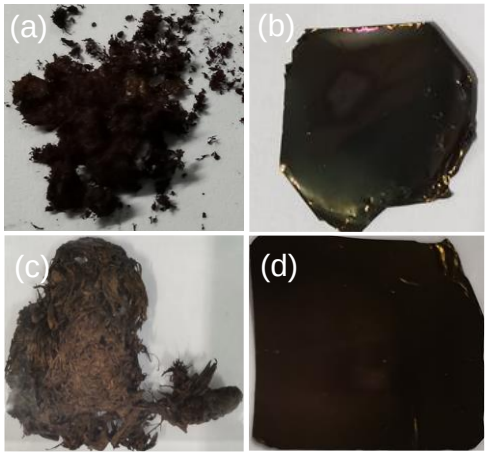

Fig. S5 Photographs of **PHCHD**$_{100}$-*b*-**PImHD**$_{50}$ (a,b) and ***d*NR**$_{x2}$-*b*-**PHCHD**$_{100}$-*b*-**PImHD**$_{50}$ (c,d).

Table S2. Characteristics for polymerization and the resultant polymers.[a]

Entry	Sample	([**HCHD**]+[**ImHD**]):[Cat][b]	Yield (%)
1	**PHCHD**$_{100}$-*co*-**PImHD**$_{50}$	(100+50):1	46
2	**PHCHD**$_{100}$-*co*-**PImHD**$_{200}$	(100+200):1	37
3	**PHCHD**$_{200}$-*co*-**PImHD**$_{100}$	(200+100):1	31

[a]Polymerization conditions: using **Ru-III** as catalyst, $CHCl_3$ as solvent, polymerization temperature = 30 °C, time = 1 h.

[b]The feed ratios of monomers to catalyst.

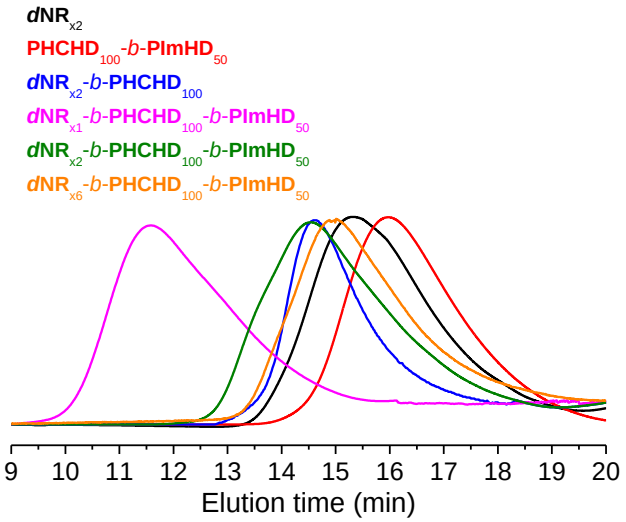

Fig. S6 GPC traces of homopolymer and block copolymers in THF.

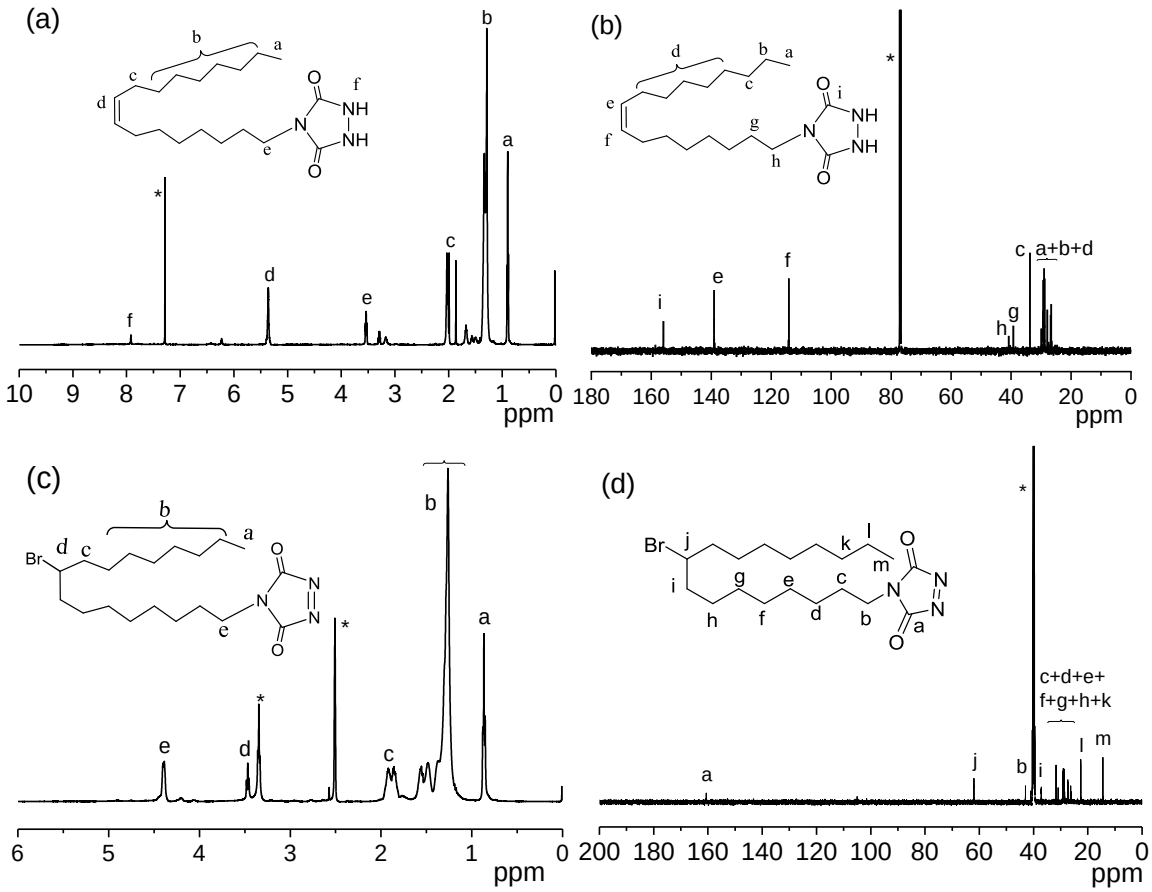

Fig. S7 ^{1}H (a,c) and ^{13}C (b,d) NMR spectra of **HD-UZ** (a,b) in $CDCl_3$ and **BrTAD** (c,d) in DMSO-d_6.

A novel TAD of 4-N-(9-bromoheptadecyl)-1,2,4-triazoline-3,5-dione (**BrTAD**) was synthesized from biobased oleic acid (OA) by the typical procedures (Scheme S2a). Conventionally, 8-ene-heptadecyl-1,2,4-urazole (**HD-UZ**) should be oxidized to the intermediate of **HD-TAD** containing alkenyl group, which would act as an AB-type

monomer and conduct self-polymerization by the *in situ* Alder-ene reaction, yielding a linear polymer **P(HD-UZ)**. Surprisingly, the oxidation of **HD-UZ** by N-bromosuccinimide (NBS) was performed in an unusual procedure accompanied with the bromo-functionalization by adding HBr to the C=C double bond of long alkenyl group to form a novel **BrTAD** containing saturated alkyl with bromide (Fig. S7).

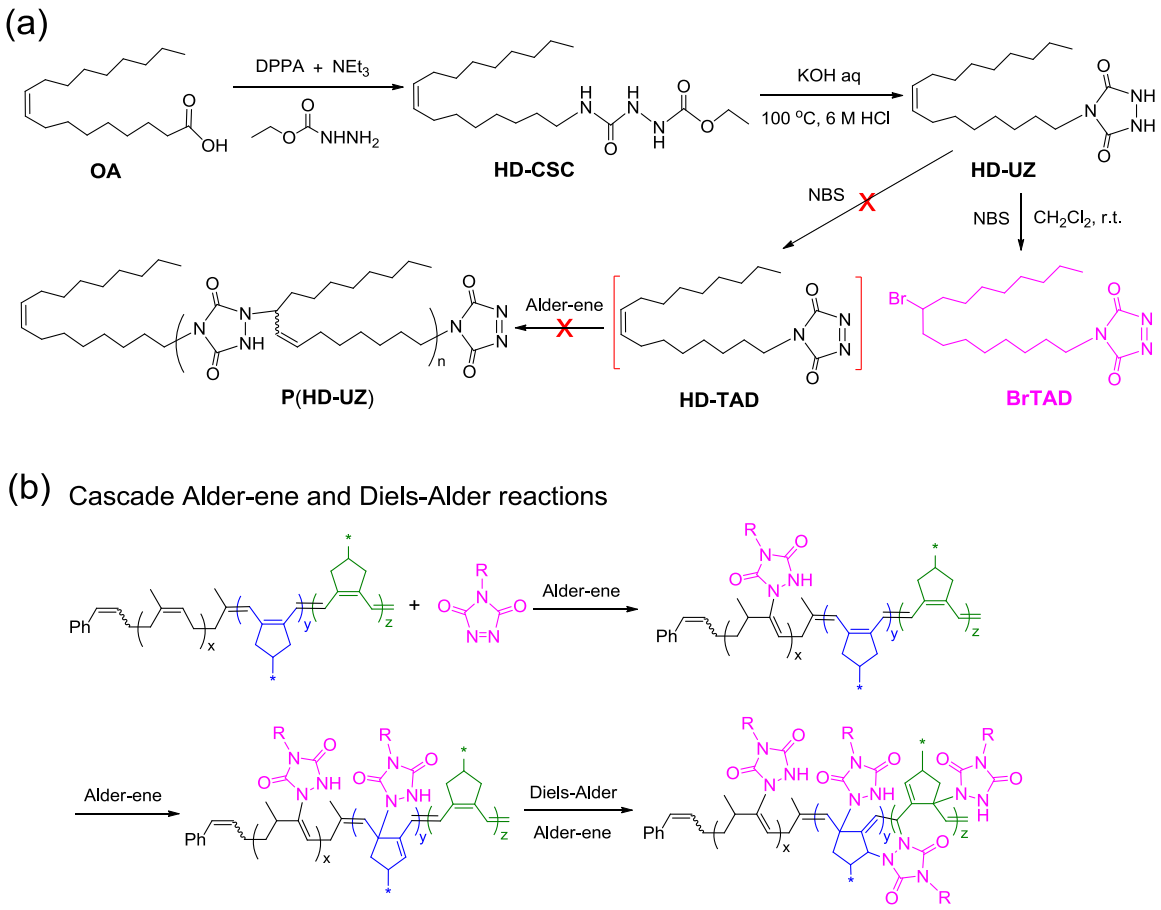

Scheme S2. Synthesis of TAD-modifier (a) and representations for cascade Alder-ene and Diels-Alder reactions of TAD with unconjugated and conjugated polymer chain (b).

Table S3. Modification of triblock copolymer by **BrTAD**.[a]

Run	Modified triblock copolymer	Feeding **BrTAD** content (mol% of double bonds)	Yield (%)
1	(***d*NR**$_{x2}$-*b*-**PHCHD**$_{100}$-*b*-**PImHD**$_{50}$)-10%**BrUZ**	0.04 mmol (10%)	90
2	(***d*NR**$_{x2}$-*b*-**PHCHD**$_{100}$-*b*-**PImHD**$_{50}$)-20%**BrUZ**	0.08 mmol (20%)	94
3	(***d*NR**$_{x2}$-*b*-**PHCHD**$_{100}$-*b*-**PImHD**$_{50}$)-40%**BrUZ**	0.16 mmol (40%)	92
4	(***d*NR**$_{x2}$-*b*-**PHCHD**$_{100}$-*b*-**PImHD**$_{50}$)-60%**BrUZ**	0.24 mmol (60%)	91
5	(***d*NR**$_{x2}$-*b*-**PHCHD**$_{100}$-*b*-**PImHD**$_{50}$)-80%**BrUZ**	0.32 mmol (80%)	89

[a]Reaction conditions: $CHCl_3$ as solvent, room temperature, time = 2 h, the total double bonds of ***d*NR**$_{x2}$-*b*-**PHCHD**$_{100}$-*b*-**PImHD**$_{50}$ = 0.4 mmol.

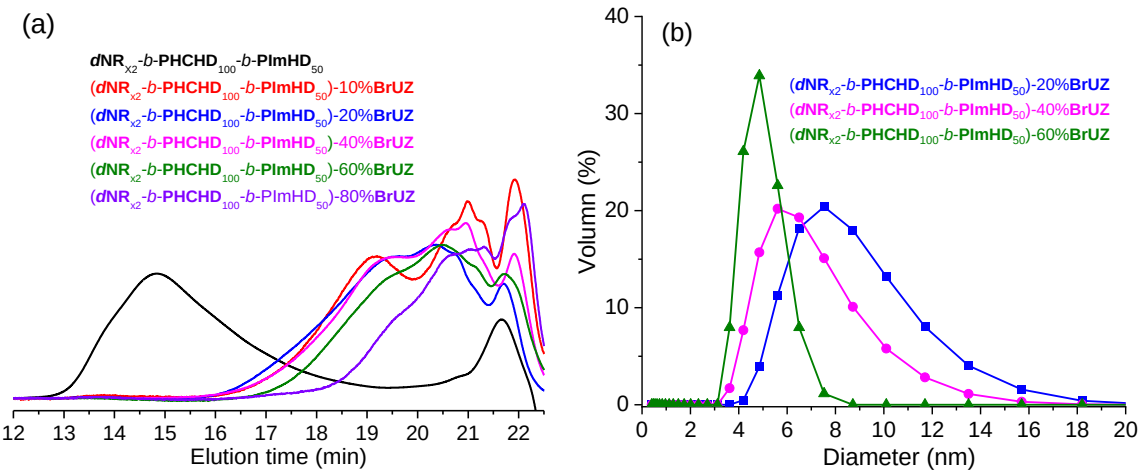

Fig. S8 GPC traces (a) and DLS diagrams (b) of modified triblock copolymers in THF.

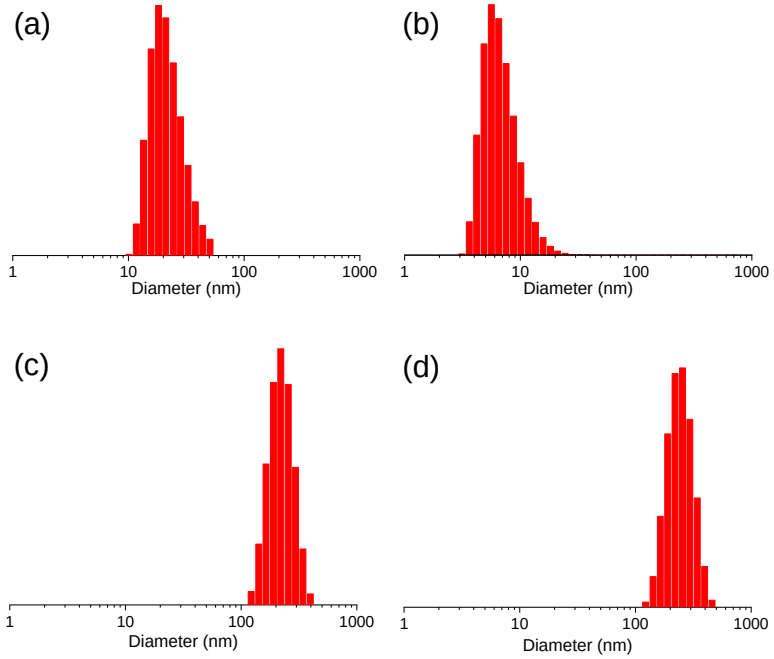

Fig. S9 DLS diagrams (a) of ***d*NR**$_{x2}$, (b) **PHCHD**$_{100}$, (c) **PHCHD**$_{100}$-*b*-**PImHD**$_{50}$, and (d) ***d*NR**$_{x2}$-*b*-**PHCHD**$_{100}$-*b*-**PImHD**$_{50}$ in THF at 1 mg mL^{-1}.

The NMR spectroscopy was an efficient method to characterize the structure of polymers. It was found that a new single signal peak of conjugated diene protons on the backbone appeared at 6.80 ppm (Figs. S10a and S10c), while the signal of the terminal alkyne protons of monomers at 2.03 ppm (Fig. S1a) completely disappeared after MCP, meaning the success for the syntheses of **PImHD** and **PHCHD**.

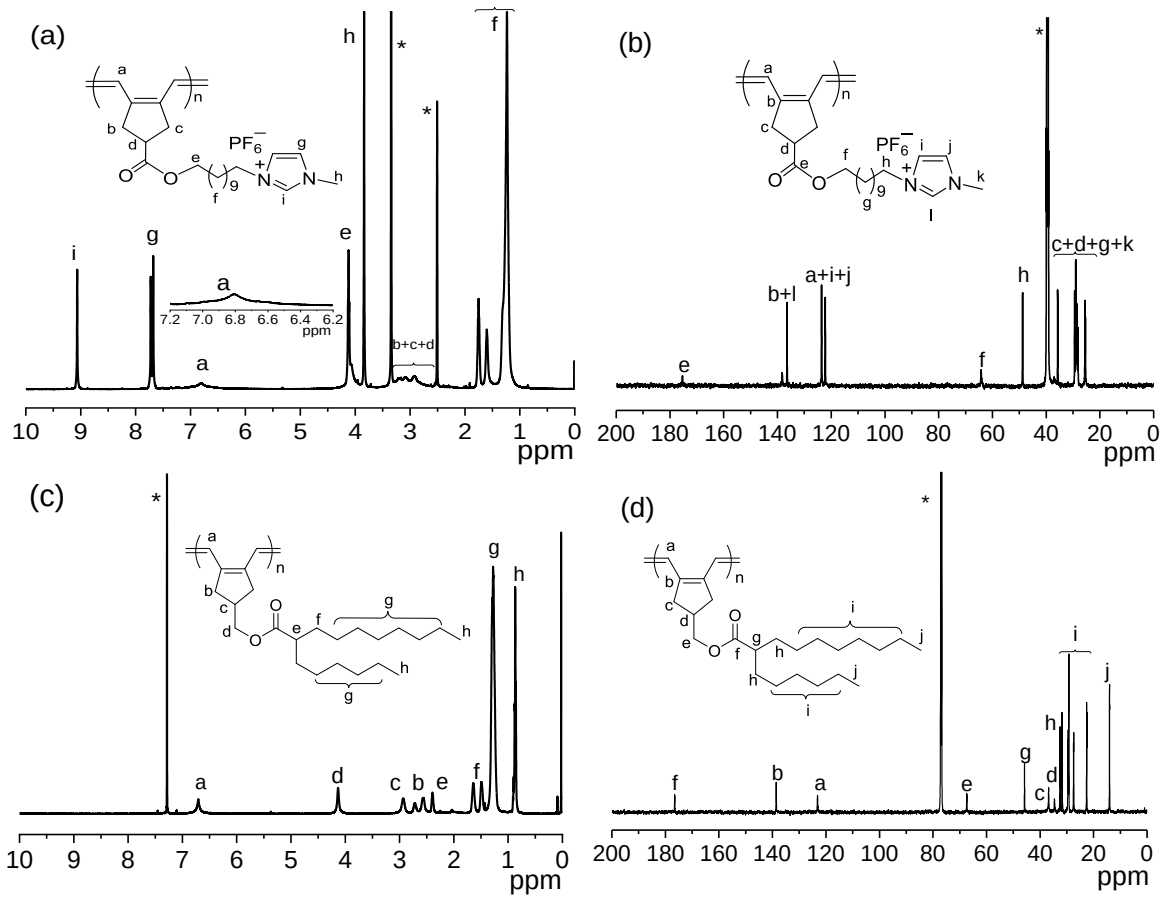

Fig. S10 ^{1}H (a,c) and ^{13}C (b,d) NMR spectra of **PImHD**$_{100}$ (a,b) in DMSO-d_6 and **PHCHD**$_{100}$ (c,d) in $CDCl_3$.

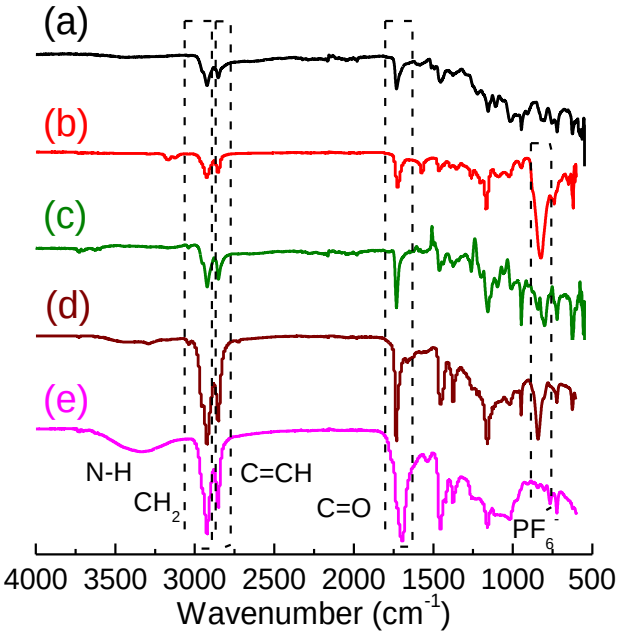

Fig. S11 IR spectra of (a) **PHCHD**$_{100}$, (b) **PImHD**$_{100}$, (c) **PHCHD**$_{100}$-*b*-**PImHD**$_{50}$, (d) ***d*NR**$_{x2}$-*b*-**PHCHD**$_{100}$-*b*-**PImHD**$_{50}$, and (e) (***d*NR**$_{x2}$-*b*-**PHCHD**$_{100}$-*b*-**PImHD**$_{50}$)-60%**BrUZ**.

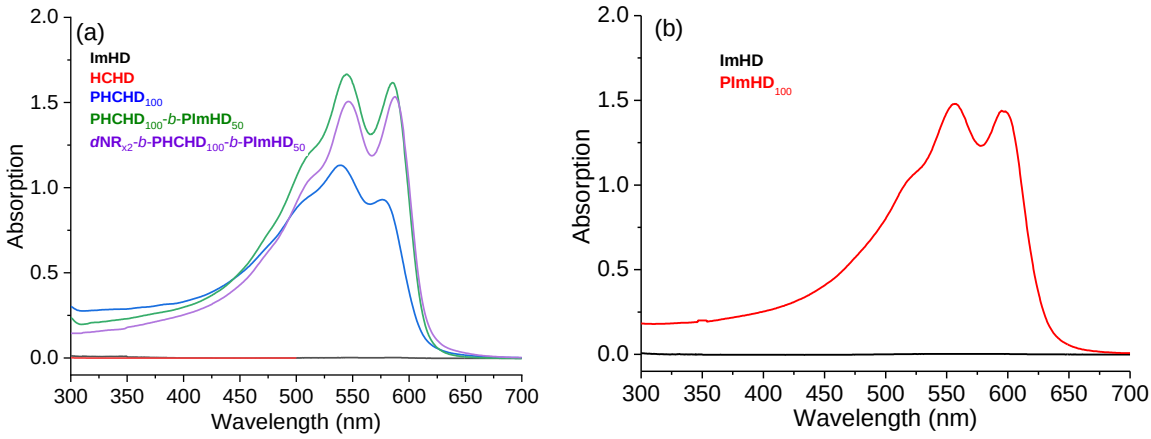

Fig. S12 UV-vis spectra of monomers and polymers in $CHCl_3$ (a) and DMSO (b) at 0.1 mg mL^{-1}.

The characterization for ***d*NR**$_{x2}$ was carried out by ^{1}H NMR and FT-IR spectroscopy. In ^{1}H NMR spectrum (Fig. S13a), three major signals appeared at 1.65, 2.0, and 5.2 ppm were assigned to methyl, methylene, and unsaturated protons of ***d*NR**$_{x2}$, respectively. Meanwhile, FT-IR spectrum of ***d*NR**$_x$ showed the typical characteristic C=C stretch band at 1640 cm^{-1}, the C-H stretching vibration at 3000~2800 cm^{-1}, and the unsaturated =C-H bending at 834 cm^{-1} for ***d*NR**$_{x2}$ structure of *cis*-PIp (Fig. S13b). Just like **PHCHD**$_{100}$-*b*-**PImHD**$_{50}$, the ^{1}H NMR analysis of triblock copolymers also revealed the characteristic proton resonances of conjugated PA backbone at 6.79 ppm in THF-d_8 (Fig. S14a), and the signals at 8.9 ppm and 7.54-7.51 ppm were from the hydrogen protons on the imidazole ring of **PImHD** block. Simultaneously, the chemical shifts at 5.17-5.10 ppm and 1.67 ppm can be assigned to the hydrogen protons on the double bonds and the methyl groups of ***d*NR**$_x$, respectively. Meanwhile, like as **PHCHD**$_{100}$-*b*-**PImHD**$_{50}$, the triblock copolymer showed the absorption bands at 2800-3100 cm^{-1} for the stretching vibration of saturated C-H bond of methylene and unsaturated C=CH bond on the conjugated backbone, and at 1731 cm^{-1} for the stretching vibration of the C=O bond on the side chain in the FT-IR spectrum (Fig. S11d). Besides, the structural characteristic absorption peak of PF_6^- in ***d*NR**$_{x2}$-*b*-**PHCHD**-*b*-**PImHD** at 834 cm^{-1} was almost coincided with the **PImHD** block of **PHCHD**$_{100}$-*b*-**PImHD**$_{50}$ at 820 cm^{-1}. Moreover, the UV-vis spectrum of ***d*NR**$_{x2}$-*b*-**PHCHD**$_{100}$-*b*-**PImHD**$_{50}$ (Fig. S12a) showed

two distinct absorption maxima at 546 nm (0-1) and 587 nm (0-0) for the conjugated **PHCHD** and **PImHD** backbones with five-membered rings in $CHCl_3$, indicating that copolymerization was processed successfully.

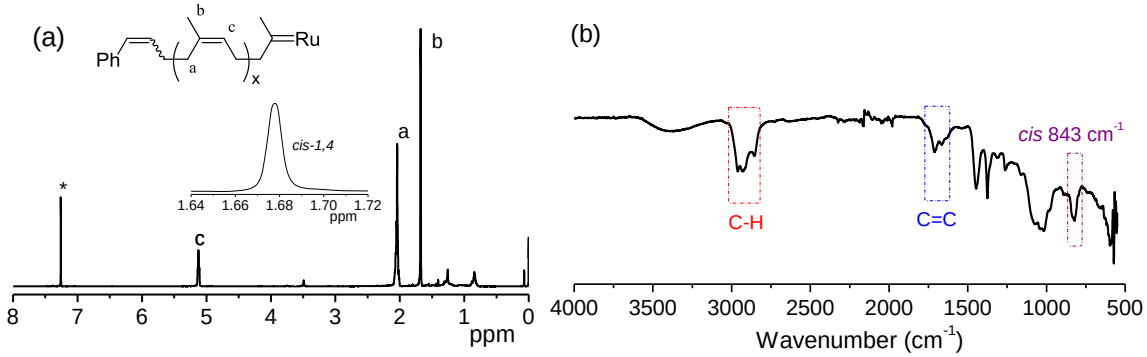

Fig. S13 ^{1}H NMR (a) and FT-IR spectra (b) of ***d*NR**$_{x2}$.

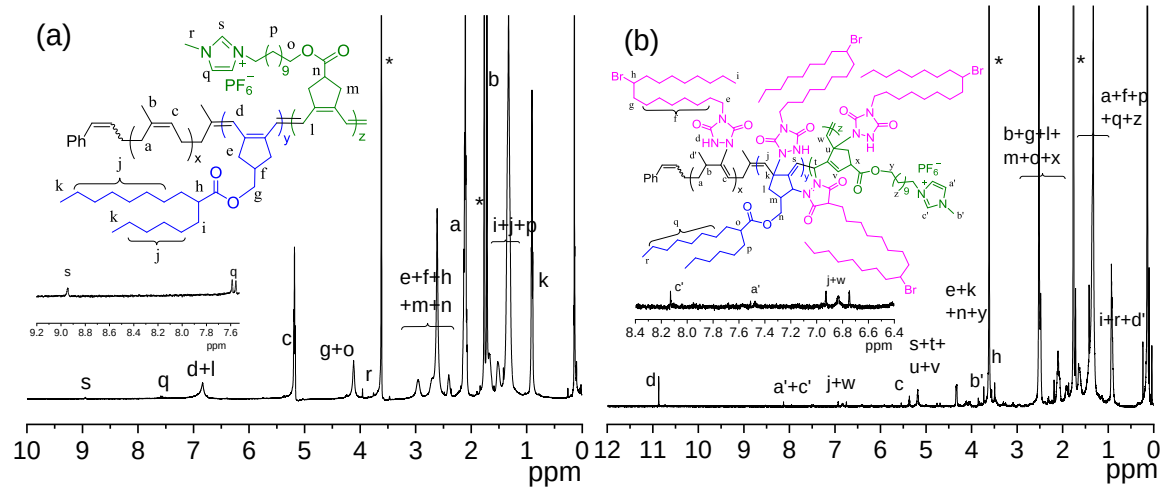

Fig. S14 ^{1}H NMR spectra of ***d*NR**$_{x2}$-*b*-**PHCHD**$_{100}$-*b*-**PImHD**$_{50}$ (a) and (***d*NR**$_{x2}$-*b*-**PHCHD**$_{100}$-*b*-**PImHD**$_{50}$)-40%**BrUZ** (b) in THF-d_8.

After modification of triblock copolymers, the original characteristic absorption weakened and significantly blue-shifted when the conjugated **PImHD** and **PHCHD** backbones were reacted with **BrTAD** in the fast cascade Alder-ene and Diels-Alder fashions, and the color change from purple to orange (see the insets of photograms in Fig. S15) was observed timely and clearly for the reaction mixture as the addition of 40%**BrTAD**, because the cascade Alder-ene and Diels-Alder reactions based on **BrTAD** would reduce the number of conjugated double bonds, and the length of conjugated polyenes in the backbone was shortened noticeably. As the ratio of **BrTAD** to double bond reached 60% and more, the

characteristic absorption of the conjugated **PImHD** and **PHCHD** backbones in (***d*NR**$_{x2}$-*b*-**PHCHD**$_{100}$-*b*-**PImHD**$_{50}$)-60%**BrUZ** and (***d*NR**$_{x2}$-*b*-**PHCHD**$_{100}$-*b*-**PImHD**$_{50}$)-80%**BrUZ** disappeared completely with the color fading to pale yellow until colorless, and thus the conjugation of **PImHD** and **PHCHD** backbones were lost wholly. In order to confirm the structure of modified triblock copolymer, ^{1}H NMR spectrum was measured as shown in Fig. S14b. The chemical shift corresponding to N-H protons (H_d) on the UZ moiety was approximately at 10.83 ppm, indicating that the Alder-ene and Diels-Alder reactions actually occurred. In addition, the FT-IR spectrum of the modified triblock copolymer displayed the stretching vibration absorption bands of saturated N-H on UZ groups at 3350 cm^{-1} (Fig. S11e), which indicated the successful post-functionalization.

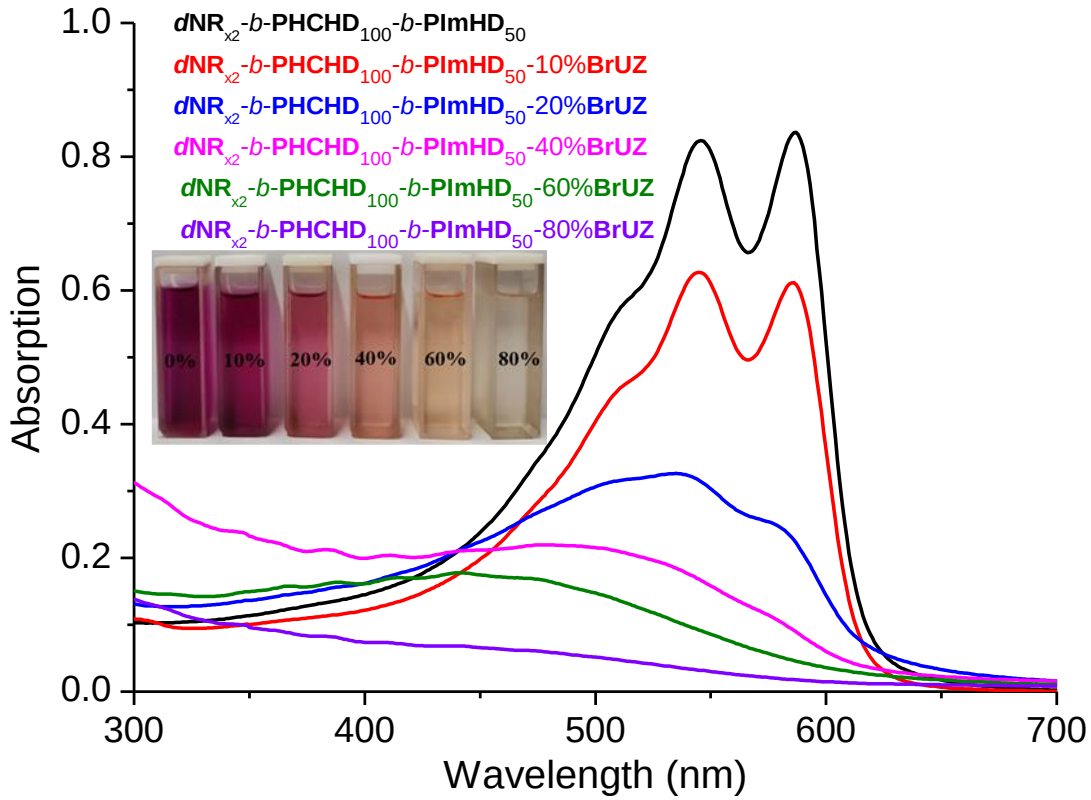

Fig. S15 UV-vis absorption spectra of modified triblock copolymers at 0.05 mg mL^{-1} in $CHCl_3$.

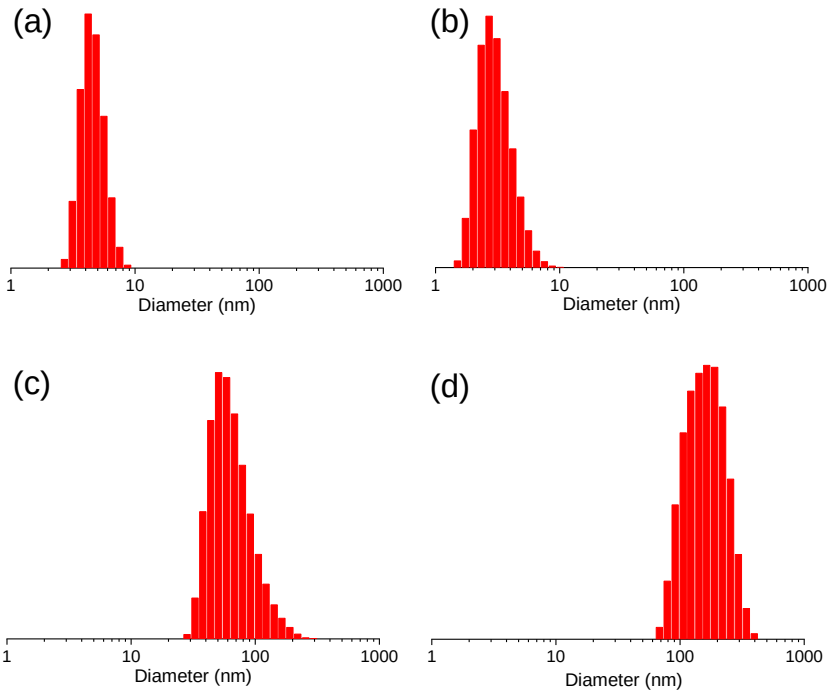

Fig. S16 DLS diagrams of (a) ***d*NR**$_{x2}$, (b) **PHCHD**$_{100}$, (c) **PHCHD**$_{100}$-*b*-**PImHD**$_{50}$, and (d) ***d*NR**$_{x2}$-*b*-**PHCHD**$_{100}$-*b*-**PImHD**$_{50}$ in $CHCl_3$ at 1 mg mL^{-1}.

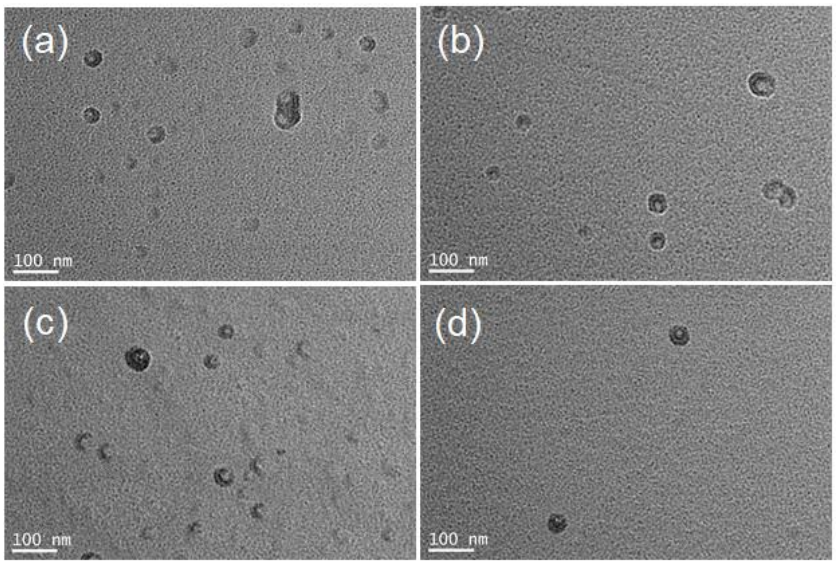

Fig. S17 TEM images of **PHCHD**$_{100}$-*b*-**PImHD**$_{50}$ (a,c) and ***d*NR**$_{x2}$-*b*-**PHCHD**$_{100}$-*b*-**PImHD**$_{50}$ (b,d) in THF (a,b) and $CHCl_3$ (c,d) at 0.0005 mg mL^{-1}.

Following the characterization of the selected simply structural diblock copolymer ***d*NR**$_{x2}$-*b*-**PHCHD**$_{100}$ by ^1H and ^{13}C NMR (Fig. 2c,d), the 2D ^1H,^1H COSY spectrum (Fig. S18a) was provided. The signals at 5.14, 2.06, and 1.68 ppm were assigned to the protons of H_c, $H_{a\text{-}a'}$, and $H_{b\text{-}b'}$ on ***d*NR**$_{x2}$ segment. Meanwhile, the signals at 6.70, 4.12, 2.91, 2.70-2.56, and 2.38 ppm belonged to the protons of H_d, H_g, H_f, H_e, and H_h on **PHCHD** segment sequentially.

Obviously, there have the cross-peak couplings between H_c with $H_{a\text{-}a'}$ and H_c with $H_{b\text{-}b'}$ (solid line in Fig. S18a), and two correlations between H_e with H_f and H_f with H_g were observed (dashed line in Fig. S18a). However, these evidences illustrated the coupling between the corresponding protons of ***d*NR**$_{x2}$ or **PHCHD** segment individually, and only the weak correlation signals between H_d with $H_{a\text{-}a'}$ and $H_{b\text{-}b'}$ appeared as reflected by the enlarged insert in Fig. S18a. Besides, 2D HMBC spectrum (Fig. S18b) was used to offer the direct information about the structural change taking place on the carbon and protons attached at the neighbor position.[S3] The HMBC analysis showed the correlations between the proton H_c with the carbons C_a and C_b (solid line in Fig. S18b), or the carbon C_c with the protons $H_{a\text{-}a'}$ and $H_{b\text{-}b'}$ (dashed line in Fig. S18b), whereas the correlations between the carbon C_d with the protons $H_{a\text{-}a'}$ and $H_{b\text{-}b'}$ were difficult to illustrate from the the enlarged insert in Fig. S18b, likely due to the C_d intensity was so weak that hardly to be detected or covered by the correlation signal of C_c. Even though the more precise structure information was not achieved from HMBC analysis, the covalent linkage between the segments ***d*NR**$_{x2}$ and **PHCHD** could be confirmed by the other results.[S4]

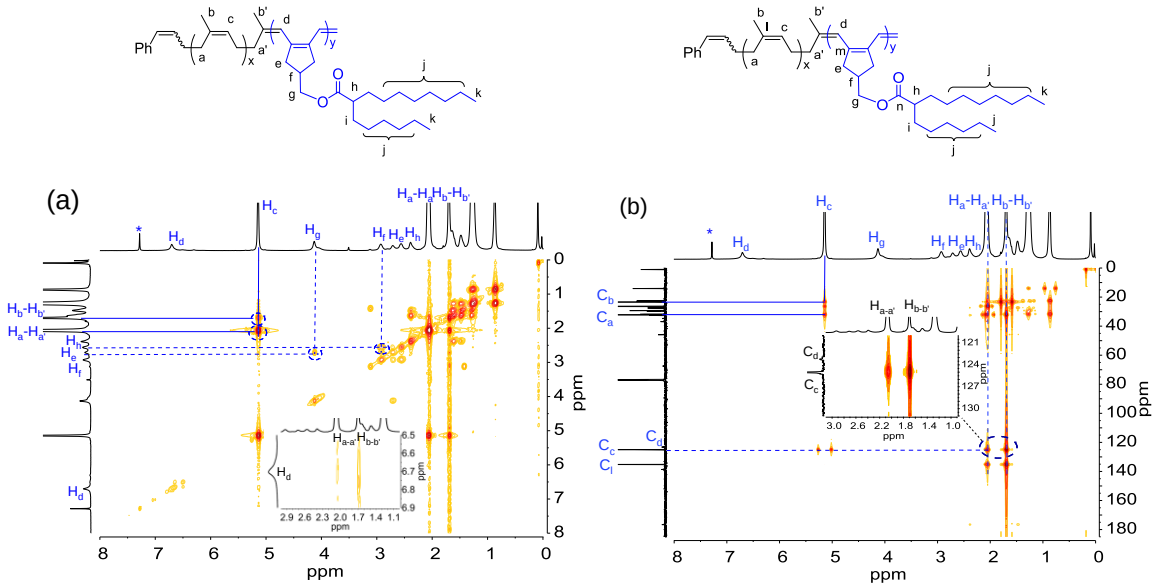

Fig. S18 ^{1}H,^{1}H COSY (a) and 2D HMBC (b) spectra of ***d*NR**$_{x2}$-*b*-**PHCHD**$_{100}$ in $CDCl_3$.

2. Thermal properties of polymers

The thermal stability of polymers was investigated by thermal gravimetric analysis (TGA). The thermal decomposition temperatures (T_d, temperature at 5% weight loss) for **PImHD**$_{100}$, **PHCHD**$_{100}$, **PHCHD**$_{100}$-*b*-**PImHD**$_{50}$, **PHCHD**$_{200}$-*b*-**PImHD**$_{100}$, and ***d*NR**$_{x2}$-*b*-**PHCHD**$_{100}$-*b*-**PImHD**$_{50}$ were 314, 308, 296, 310, and 270 °C sequentially (Fig. S19a), indicating these polymers had good thermal stability. The T_ds for (***d*NR**$_{x2}$-*b*-**PHCHD**$_{100}$-*b*-**PImHD**$_{50}$)-X%**BrUZ** (X=10, 20, 40, 60, and 80) were 236, 232, 215, 214, and 202 °C in turn (Fig. S20a), which were lowered than that of urazole groups-contained polymers (around 300 °C),[S1] and decreased along with the increase in degree of TAD-modification to ***d*NR**$_{x2}$-*b*-**PHCHD**$_{100}$-*b*-**PImHD**$_{50}$. The glass transition temperature (T_g) of polymers was tested by differential scanning calorimetry (DSC), and the T_gs for **PImHD**$_{100}$, **PHCHD**$_{100}$, **PHCHD**$_{100}$-*b*-**PImHD**$_{50}$, **PHCHD**$_{200}$-*b*-**PImHD**$_{100}$, and ***d*NR**$_{x2}$-*b*-**PHCHD**$_{100}$-*b*-**PImHD**$_{50}$ were 7, 13, 2, 3, and -64 °C (Fig. S19b), separately. The T_gs for (***d*NR**$_{x2}$-*b*-**PHCHD**$_{100}$-*b*-**PImHD**$_{50}$)-X%**BrUZ** (X=10, 20, 40, 60, and 80) appeared at -55, -49, -33, -23, and -18 °C (Fig. S20b) were gradually rose as the increase in the number of incorporated polar group **BrUZ**. It was believed that the enhanced intra- and inter-molecular hydrogen bond interactions between the –NH groups decreased the free volume, and the rotation of polymer chain needed higher temperature to overcome energy barrier, resulting in an increased T_g.[S2]

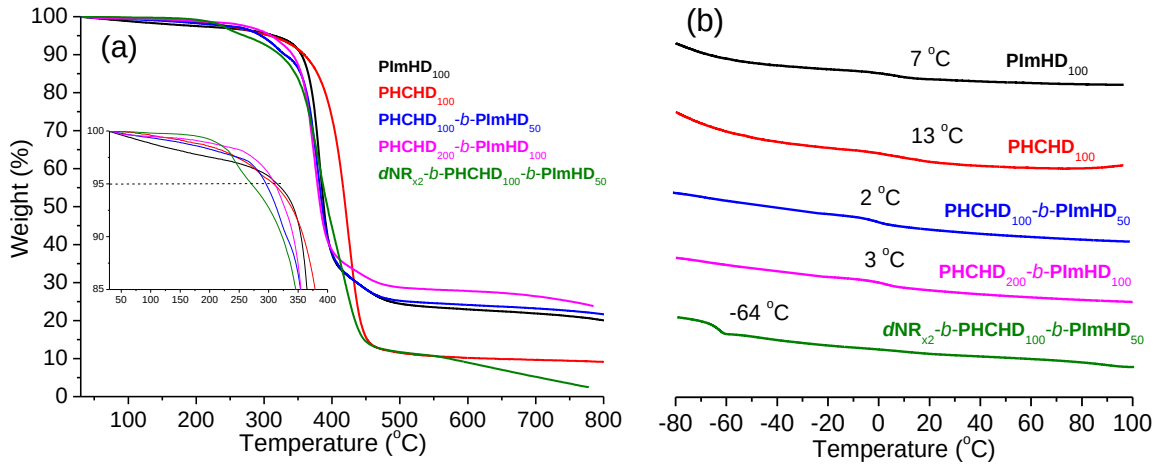

Fig. S19 TGA (a) and DSC (b) curves of homopolymers and block copolymers.

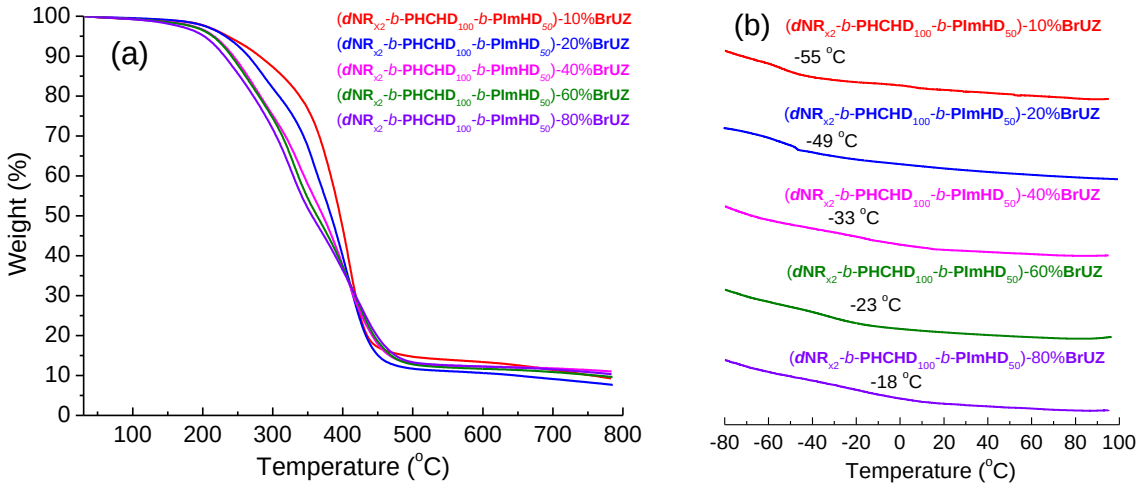

Fig. S20 TGA (a) and DSC (b) curves of modified triblock copolymers by different amounts of modifier.

3. Dynamic mechanical properties of triblock copolymers

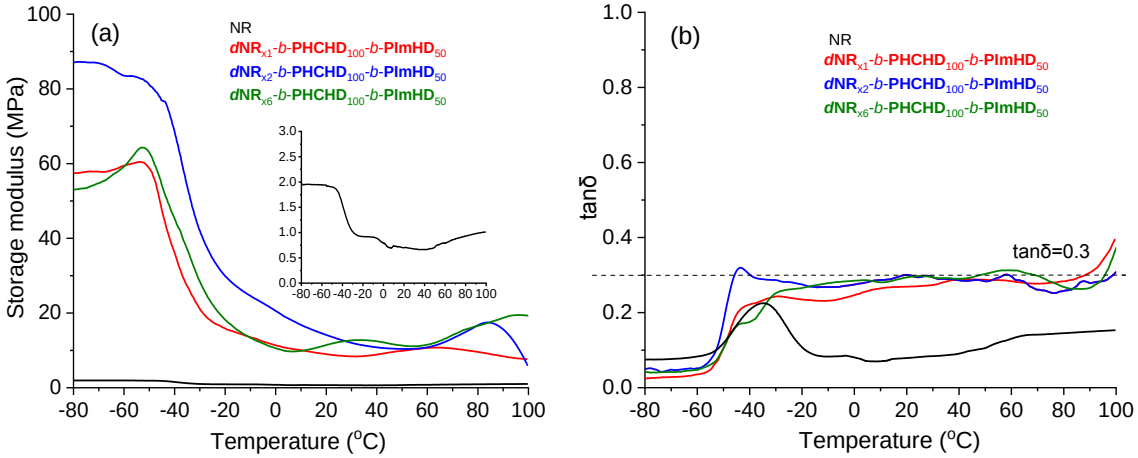

Fig. S21 Dependence of *E*' (a) and tan*δ* (b) on temperature for ***d*NR$_x$-*b*-PHCHD$_{100}$-*b*-PImHD$_{50}$**.

References

S1. K. S. D Bruycker, S. Billiet, H. A. Houck, S. Chattopadhyay, J. M. Winne and F. E. D. Prez, *Chem. Rev.*, 2016, **116**, 3919.

S2. H. Li, Q. Ren, J. Chen, H. Zhang, J. Wu and M. Xie, *React. Funct. Polym.*, 2018, **132**, 104-111.

S3. A. Herrera, E. F. Valle, E. M. Gutiérrez, R. M. Álvarez, D. Molero, Z. D. Pardo and E. Sáez, *Org. Lett.*, 2010, **12**, 144-147.

S4. Y.. Phuphuak, F. Bonnet, G. Stoclet, M. Bria and P. Zinck, *Chem. Commun.*, 2017, **53**, 5330-5333.